FINGERING IN 2-DIMENSIONAL HOMOGENEOUS UNSATURATED POROUS MEDIA

Nobuyuki Tamai, Professor., Takashi Asaeda, Assoc. Prof.
Charles.G.Jeevaraj, Grad. Stud., Yasuharu Tanaka, Grad. Stud.
University of Tokyo

1. INTRODUCTION: The unsaturated ground water zone acts as a link between the rainfall infiltration and the saturated ground water zone. It is suspected that infiltration takes place through preferential paths which become the real link transporting the water to the deeper stratum. Since in the present infiltration theory it is assumed that water front moves stable until it reaches the saturated zone, it is essential to investigate the real pattern of motion through porous medium. In this study an attempt is made to clarify the moving pattern of the front when the infiltration takes place through the unsaturated homogeneous medium. One of the first demonstrations of unstable fingering phenomena in a Hele- Shaw cell is due to Saffman & Taylor.[5] They established a stability criteria and later Chuoke et al.[1] improved it including interfacial tension. From the previous studies it is also understood that there exists a clear difference between the shape of the fingers developed in Hele-Shaw cell and the porous medium. Considering the infiltration of water through initially unsaturated medium, Hill & Parlange[4] have experimentally demonstrated the formation of finger when the water front enters from finer medium to coarser medium and was mentioned that the front in homogeneous medium is stable. But this is only true when there exists a continuous water supply at the top surface of the medium as it was the case in their experimental set up. In a practical sense, a continuous supply can only be found in artificial recharge by flooding. Otherwise the supply would be mostly discontinuous and thus an air phase

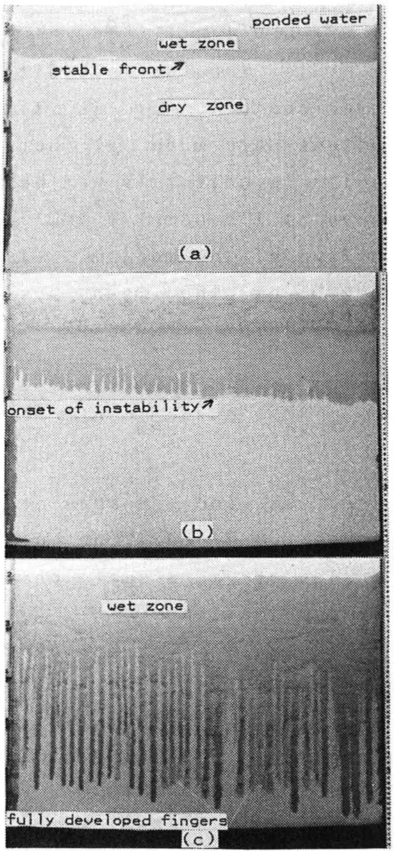

Fig. 1. Experimental observation.

is entrained through the top of the medium and fingers develop during redistribution. In the experiments a homogeneous medium is used by which the other possible factors which can contribute to fingering is avoided.

2. EXPERIMENT ON DRY MEDIUM: Two parallel glass panels were closely spaced to make up a gap of 0.25cm and a rectangular region of 76cmx50cm is used for experiment. Brass net was used at the bottom for the free escape of air. The gap was packed with dry homogeneous glass beads of uniform size and the liquid of known volume was input using a 76cm long rectangular vessel. The liquid immediately got ponded up on top of the medium while infiltration was taking place and a stable front moved down as in Fig.1(a) until the ponded liquid on the top surface entered into the medium. As soon as the liquid entered instability started to appear and gradually grew into fingers, [Figs.1(b)&(c)] and later infiltration was only through these fingers. Timed photography was used to trace the motion of the front.

3. STABILITY ANALYSIS: 1)<u>Theory</u>: For the infiltration through initially unsaturated zone, the Richard's equation is

$$\nabla [K \nabla \Phi] = \frac{\partial \theta}{\partial t} \tag{1}$$

Where K is the permeability, Φ is the velocity potential, θ is the moisture content, t is time. For the present problem following assumptions are made. a) There exists a distinct wetting front and the soil is uniformly wet behind the front and having constant K and θ and hence Eq.1 becomes $\nabla^2\Phi=0$. b)$L>>\xi$, where L is the depth of front from the surface of the medium. ξ is the displacement of the front from mean. Taking z=0 at the mean position, the boundary conditions are

$$\frac{\partial \xi}{\partial t} = [-\frac{\partial \Phi}{\partial z}]_{z\xi} \quad (2) \qquad \mathrm{Lim.}_{z\to-\infty}[\frac{\partial \Phi}{\partial z}] = 0 , \quad (3)$$

and

$$\Delta p \,]_{z=\xi} = \sigma(-\frac{\partial^2 \xi}{\partial x^2} - \frac{\partial^2 \xi}{\partial y^2}) , \tag{4}$$

where Δp is the pressure drop at the front, σ is the surface tension. Using Eqs.2 & 3, Eq.1 can be solved by seperation of variables, where ξ is considered as a small perturbation from the mean and expressed as a Fourier combination

$$\xi = \varepsilon_0 \exp[nt+i(\alpha_x x+ \alpha_y y)] \tag{5}$$

where ε_0 is amplitude, n is growth rate, t is time elapsed and α is wave number($\alpha^2=\alpha_x^2+\alpha_y^2$). Therefore solution for Eq.1 can be written as (for $\alpha\xi<<1$)

$$\Phi = -\frac{n}{\alpha}\varepsilon_0 \exp[\alpha z+nt+i(\alpha_x x+\alpha_y y)]. \tag{6}$$

Along the front $\Delta p]_{z=\xi} = \frac{\mu_1}{k_1}([\Phi]_{z=\xi} - W\xi) + \rho_1 g\xi$. (7)

Using Eqs.4 to 7 the following can be obtained.

$$n = [\rho_1 g k_1/\mu_1 - W]\alpha - \sigma\alpha^3 k_1/\mu_1 . \tag{8}$$

For the front instability $n>0$ and hence $\alpha<\alpha_c$, where

$$\alpha_c = \left[\frac{\mu_1}{k_1 \sigma} \left(\frac{\rho_1 g k_1}{\mu_1} - W \right) \right]^{1/2} \tag{9}$$

where μ_1, ρ_1 and k_1 are absolute viscosity, density and intrinsic permeability respectively. W is the Darcy's velocity of the front. From Eq. 8 the wave number which gives maximum growth rate, (from $\frac{\partial n}{\partial \alpha}=0$) is

$$\alpha_m = \alpha_c/\sqrt{3}. \tag{10}$$

Therefore, from Eq. 9 the condition for instability is

$$W < \frac{\rho_1 g k_1}{\mu_1} \tag{11}$$

2) <u>A Qualitative Analysis on Experimental Results:</u>

Observation 1: "The front was stable as long as a ponded liquid remained on top (Fig. 2(a))". Under the assumptions mentioned earlier, the front velocity is

$$W = \frac{\rho_1 g k_1}{\mu_1} \left(1 + \frac{h_0 + C_f}{L(t)} \right), \tag{12}$$

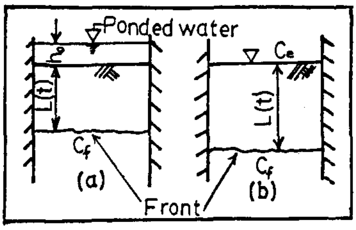

Fig. 2. Illustration on infiltrating front.

where h_0 is the height of ponded water and C_f is the head due to surface tension at the front. L(t) is the depth of front from the surface of the medium. Since (h_0+C_f) is positive, from Eq. 12 $W>\rho_1 g k_1/\mu_1$.

Observation 2: "Front become unstable as soon as the ponded liquid vanishes. (Fig. 2(b))". For this case, it can be written similar to Eq. 12 as

$$W = \frac{\rho_1 g k_1}{\mu_1} \left(1 + \frac{C_f - C_e}{L(t)} \right) \tag{13}$$

where C_e is the head due to surface tension created by the air entry from top surface of the medium. According to Dussan V.[2]: "The contact angle of the liquid with solid grains is generally smaller in receding side than advancing side". Therefore, generally $C_f<C_e$ and hence from Eq. 13 $W<\rho_1 g k_1/\mu_1$ and thus the front become unstable and fingers develop.

3) <u>Quantitative Analysis on the Experimental Observation:</u>

In the experimental results, the wave length (λ_{obs}) can be measured as the distance between consecutive troughs. The wave length (λ_m) which gives the maximum growth rate can be obtained from Eq. 10 as $\lambda_m = 2\pi/\alpha_m$. Fig. 3 shows the appropriateness of the theory in comparison with the experimental results. In a nondimensional form Eq. 8 can be expressed as $\bar{N} = \bar{\alpha} - \bar{\alpha}^3/12$, where $\bar{\alpha} = [12k_1\sigma/(\mu_1(W-\rho_1 g k_1/\mu_1))]^{1/2}\alpha$; and $\bar{N} = [12k_1\sigma/(\mu_1(W-\rho_1 g k_1/\mu_1))]^{1/2}/(W-\rho_1 g k_1/\mu_1)n$. Fig. 4 shows fairly good agreement regarding the growth rate of fingers between the experimental results and the above expression.

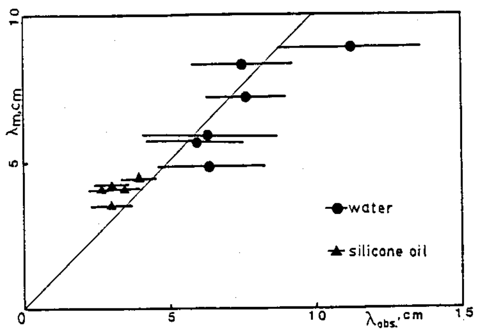

Fig. 3. Wave length compared.

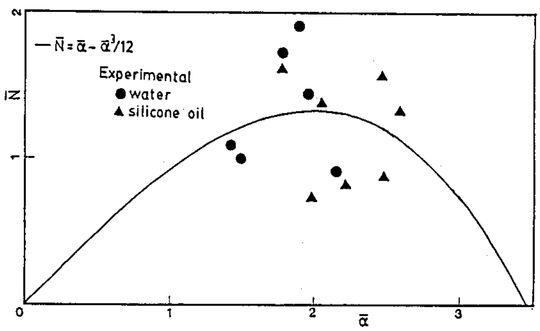

Fig. 4. Initial growth rate compared.

4. MODELLING THE POROUS MEDIUM: Sinusoidal Porous Path Model.

To understand the mechanism of finger growth, the medium can be represented by a number of vertical axisymmetric tubes with sinusoidally varying diameter in the axial direction as in Fig. 5. As this path incorporates the convergent-divergent characteristic of the actual porous medium, it is a reasonable choice than a circular straight capillary representation. Let $r_0(z)=a-\delta\cos(2\pi z/W_\lambda)$ be the radius of the porous path . The dimension of a sinusoidal unit is determined from the measurable properties such as porosity, average grain size etc., using the following eqs..

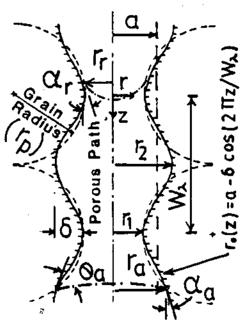

Fig. 5. Sinusoidal unit.

$$W_\lambda \approx 2r_p \; ; \; r_1=0.155+\frac{(0.414-0.155)}{(0.476-0.26)}(p_\varepsilon-0.26) \; , \qquad (14)$$

$$p_\varepsilon(1-S_w)8r_p^3=2r_p\pi(a^2+\delta^2/2), \qquad (15) \qquad\qquad r_1=a-\delta;\; r_2=a+\delta \; , \qquad (16)$$

where Eq. 14 is an inference from packing of spheres and Eq. 15 denotes that the available pore space is constructed with a sinusoidal unit.

Even in this highly simplified axisymmetric flow situation the Navier-Stokes equation for the motion of a small column of liquid cannot be solved exactly unless some assumptions are made, such as a) inertial effects are negligible (small velocities), b) movement is steady within a small time step and c) pressure is assumed to be invariant over a cross section. The Navier-Stokes equation within a time step is

$$F_z - \frac{\partial p}{\partial z} + \mu\left(\frac{\partial^2 w}{\partial r^2} + \frac{1}{r}\frac{\partial w}{\partial r} + \frac{\partial^2 w}{\partial z^2}\right) = 0 \; , \qquad (17)$$

The boundary conditions are

$$v = w = 0 \quad \text{at} \quad r = r_0 \qquad (18)$$

$$v = \frac{\partial w}{\partial r} = 0 \text{ at } r = 0 \qquad (19)$$

and $\quad v(r,z)=v(r,z+W_\lambda);\quad w(r,z)=w(r,z+W_\lambda) \qquad (20)$

where a is mean radius, δ is the wave amplitude about mean, W_λ is wave length, w, v are velocities in z, r directions respectively, p is the pressure, μ is the viscosity, F_z is the body force per unit volume. Assuming that at each section the sectional average velocity $(\hat{w})$ can be expressed by,

$$w = 2\hat{w}[1-r^2/r_0^2(z)] \tag{21}$$

Using Eq. 18 to 21, Eq. 17 can be reduced in terms of measurable quantities as

$$\mu S_g V_0/a^2 W = \rho g V_0 - 2\Pi\sigma[r_r \cos\alpha_r - r_a \cos(\theta_a - \alpha_a)] \tag{22}$$

where W is the average velocity of the moving liquid column, V_0 is the volume of liquid in a porous path, σ is the surface tension, a, r_r, r_a, θ_a, α_a and α_r are shown in Fig. 5. S_g is the shape factor: Ratio of resistance given by a path of varying cross section to the cylindrical path, which can be estimated as follows: For a liquid continuously flowing through this porous path, the equation of motion for the creeping flow in terms of stream function is

$$E^4\psi = 0 \text{ , where } E^2 = \frac{\partial^2}{\partial z^2} + \frac{\partial^2}{\partial r^2} + \frac{1}{r}\frac{\partial}{\partial r} \ . \tag{23}$$

Boundary conditions

$$\partial\psi/\partial z = 0 \quad \text{at } r = 0, \tag{24}$$

$$\partial\psi/\partial z = \partial\psi/\partial r = 0 \text{ at } r = r_0(z), \tag{25}$$

$$\int_0^{r_0(z)} r\frac{\partial\psi}{\partial r}\, dr = W a^2/ 2 \ , \tag{26}$$

and

$$\psi(r, z) = \psi(r, z+W_\lambda), \tag{27}$$

The following solution satisfy Eq. 23 to 27,

$$\psi = Wa^2[r/r_0(z) - 0.5[r/r_0(z)]^2] \tag{28}$$

pressure drop (Δp_λ) over a wave length W_λ is

$$\Delta p_\lambda = \int_0^{W_\lambda} \frac{\partial p}{\partial z}\, dz + \int_0^{r_0(z)} \frac{\partial p}{\partial r}\, dr = 8\mu\, Wa^2 \int_0^{W_\lambda} dz/[r_0(z)]^4 \tag{29}$$

where for circular straight path with radius equal to the mean radius of the above sinusoidal path, the pressure drop Δp^*_λ over a length W_λ is

$$\Delta p^*_\lambda = 8\mu W.W_\lambda/a^2 . \text{ Hence } S_g = \Delta p_\lambda/ \Delta p^*_\lambda = a^4/W_\lambda \int_0^{W_\lambda} [1/r_0(z)^4] dz. \tag{30}$$

5. MECHANISM OF LATERAL FLOW BETWEEN NEIGHBORING PORES. It is assumed that the vertical sinusoidal paths are laterally connected through nozzle-like units (Fig. 6a) and the flow through it can be estimated.[3]

$$q = \Delta p_d\, C_t^3/(3\mu)\ [1 + 2\, \xi_0]\ [1 - \xi_0]^2 \tag{31}$$

where C_t is the radius of throat. Δp_d is the average pressure diference across this nozzle-like unit. Considering the negative pressure due to air-water menisci, the pressure gradient between two neighboring porous paths can be assumed to be, (Fig. 6b)

$$\Delta p_d = \frac{1}{2}[x_1 - x_2]\ [z/h_a + 1 - (h_a - z)/h_b] \tag{32}$$

with x_1, x_2, z, h_a and h_b as shown in Fig. 6b.

6. RESULTS AND DISCUSSION. Thus a simulation is carried out using the sinusoidal porous paths including the lateral sharing basing on Eq. 32. Initially the front is assumed to be perturbed with the wave number obtained from the stability analysis. Fig. 7 & 8 show one of the simulated and the corresponding observed results respectively and hence comparing these it can be said that the lateral flow due to pressure difference between porous paths is one of the possible mechanism which makes the fingers to grow.

7. CONCLUSION: It is experimentally evident that even in a homogenous medium the water is transported through fingers during redistribution. Considering the experimental uncertainties the stability analysis gives a reasonable prediction on the spacing of the fingers. The pressure difference created between the neighboring pores due to the air-water menisci is a possible mechanism in accumulating the water to be transported towards the fingers.

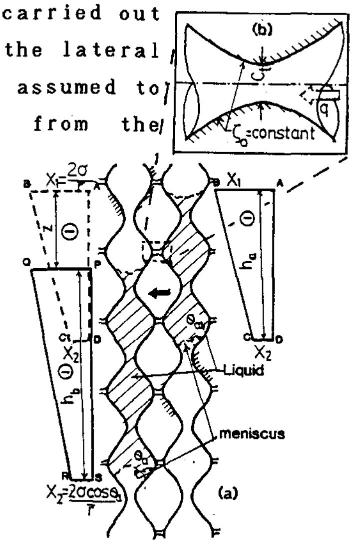

Fig. 6. Lateral sharing between pores.

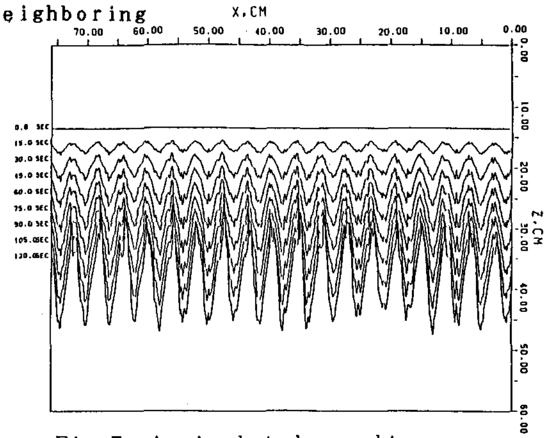

Fig. 7. A simulated result.

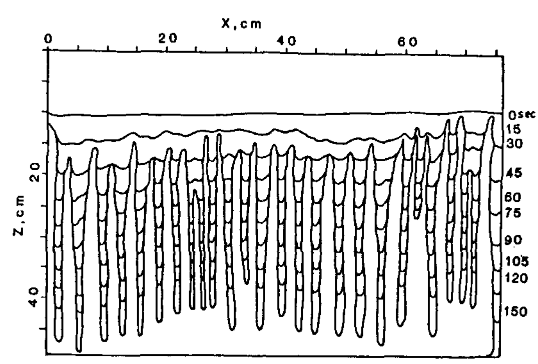

Fig. 8. A tracing of observed fingers.

References:

1. Chuoke, R. L, van Meurs, P. & van der Poel. C, Trans. AIME, 216, pp. 183-, 1959.
2. Dussan V, E. B, Ann. Rev. Fluid Mech., 11, pp. 371-400, 1979.
3. Happel, J and Brenner, H, Low Reynolds Number Hydrodynamics, Prentice Hall, Inc., 1965.
4. Hill, D. E. and Parlange, J. Y, Soil Sci. Soc. Am., 36 pp. 697-702, 1972.
5. Saffman, P. G. and Taylor, G. I. Proc. Roy. Soc. A, 245 pp. 312-329. 1958.